Self-consistent calculations of edge channels in laterally confined two-dimensional electron systems

Karlheinz Lier
Physikalisches Institut, Universität Würzburg, D-97074 Würzburg, Federal Republic of Germany

Rolf R. Gerhardts
Max-Planck-Institut für Festkörperforschung, Heisenbergstrasse 1, D-70569 Stuttgart, Federal Republic of Germany
(Received 26 January 1994)

We calculate the distribution of incompressible and compressible regions at an electrostatically defined edge of a two-dimensional electron system (2DES) in a strong perpendicular magnetic field B for two models, one with a strictly 2D arrangement of gate and charges, and one with a realistic 3D structure. We ensure electrochemical equilibrium by self-consistent calculation of the electrostatic potential from the electron density and the boundary conditions defined by the metallic gates, and of the electron density in this potential, using the Thomas-Fermi approximation. Both models yield qualitatively the same results. In the limit of zero temperature and strong magnetic field, and at distances from the edge which are much larger than the effective Bohr radius, our 2D model yields quantitatively the same result for the density profile in the 2DES as recent work by Chklovskii, Shklovskii, and Glazman, who considered a purely electrostatic model, without requiring electrochemical equilibrium for $B = 0$. We demonstrate explicitly how the incompressible regions are destroyed with increasing temperature.

I. INTRODUCTION

The concept of edge states has been used very successfully in describing many properties of mesoscopic two-dimensional electron systems (2DES) under conditions of the quantum Hall effect. In its single-particle version for noninteracting electrons, it provides the basis of the Landauer-Büttiker formalism,[1] which has been applied with great success to understand magnetoresistance measurements on mesoscopic samples,[2–5] in particular on those with complicated geometry and distribution of filling factors, produced by special arrangements of gates.[6] The validity of this concept has been established by many experiments, as has been discussed in several review articles.[2–5] Some recent experiments[7,8] seem to indicate, however, that the single-particle version of this concept is not sufficient and that many-body effects such as screening of slowly varying electrostatic fields by the interacting 2DES must be incorporated.

In a strong perpendicular magnetic field B, the screening properties of a 2DES are very nonlinear, as has been pointed out by analytical[9] as well as by numerical[10,11] calculations within the Hartree approximation. If the electrostatic potential energy $V(\mathbf{r})$ of an electron varies smoothly in the plane of the 2DES, i.e., on a characteristic length d much larger than the magnetic length $l_m = (c\hbar/eB)^{1/2}$, then screening leads to a pinning of the energy bands at the Fermi level,[10] accompanied by spatial regions where the screened potential is flat (perfect screening).[12] Under these conditions ($l_m \ll d$), the spatial extent of the wave functions can be neglected on the scale d and the Hartree approximation reduces to the Thomas-Fermi approximation (TFA) with the local relation

$$n_s(\mathbf{r}) = \int dE\, D(E)\, f([E + V(\mathbf{r}) - \mu]/k_BT) \qquad (1.1)$$

between the density $n_s(\mathbf{r})$ of the 2DES and $V(\mathbf{r})$. Here $f(\epsilon) = [1 + \exp(\epsilon)]^{-1}$ is the Fermi function, μ the (spatially constant) electrochemical potential, T the temperature, and

$$D(E) = \frac{g_s}{2\pi l_m^2} \sum_{j=0}^{\infty} \delta(E - \hbar\omega_c(j + \tfrac{1}{2})) \qquad (1.2)$$

the Landau density of states with $\omega_c = eB/m^*c$ the cyclotron frequency; $g_s = 2$ takes into account the spin degeneracy. This local relation leads in the limit of zero temperature to a simple real-space picture of screening, as has been emphasized by Luryi[12] and by Efros:[13,14] the area occupied by the 2DES can be divided into two types of regions, "compressible" regions in which one of the Landau bands is pinned at the Fermi level and screening is perfect, since electrons can easily be redistributed between available states, and "incompressible" regions in which the Fermi energy falls into a gap between (or below) the Landau bands and which do not contribute to screening since a redistribution of electrons is energetically impossible. In these incompressible regions the electron density $n_s(\mathbf{r})$ is constant while $V(\mathbf{r})$ varies, whereas in the compressible regions $n_s(\mathbf{r})$ varies and $V(\mathbf{r})$ is constant. Recently Chklovskii, Shklovskii, and Glazman[15] (CSG) have shown that this simplified picture of screening can be exploited to develop, for sufficiently simple geometries, an *analytical* theory of screening in strong magnetic fields.[15,16]

In order to obtain explicit analytical results for the screened potential and the density profile of the screening 2DES, CSG had to rely on two somewhat oversimplifying model assumptions. First, a real sample with a metal gate at some distance L from the plane of the 2DES and positive space charges behind a spacer is replaced by a model with a strictly two-dimensional distribution of charges in the (x-y) plane of the 2DES. This is thought to be a good approximation, if L is negligible on the length scale d. For typical experimental situations one has, however, only $L/d \sim 0.2$.[15] The second critical assumption is that, even for vanishing magnetic field, the 2DES shows perfect metallic screening, so that $\nabla V(\mathbf{r}) = 0$ where the density of the 2DES is finite, $n_s(\mathbf{r}) \neq 0$. To be specific, CSG consider a model with translational invariance in the y direction: a metallic gate in a half plane (say $x < 0$), a background of positive charge density en_0 in the other half plane ($x > 0$), and the 2DES with density $n_s(x)$ (in $x > d$) separated from the in-plane gate by a depletion layer of width d and approaching the background density at infinity [$n_s(x) \to n_0$ for $x \to \infty$]. Since the 2D density of states for $B = 0$ is constant, $D(E) = D_0\theta(E)$, with $D_0 = m^*/\pi\hbar^2$ and $\theta(x)$ the unit step function, one expects within the TFA for $T = 0$ that $n_0 = D_0 E_F$ and

$$[n_0 - n_s(x)] = D_0 V(x)\,. \tag{1.3}$$

This requirement of electrochemical equilibrium is not satisfied in the CSG theory. Instead, CSG follow an argument by Glazman and Larkin,[17] who have demonstrated that, for $V(0) \gg E_F$, the electron density varies on the scale of the depletion length d. Then, according to the self-consistency requirement (1.3), the gradient of the screened potential inside the 2DES is of the order $dV/dx \sim E_F/d$, which is much smaller than the potential gradient in the depletion layer $dV/dx \sim V(0)/d$. Glazman and Larkin argue that the self-consistent problem may be solved by a kind of perturbation expansion in the small parameter $E_F/V(0)$ and that, to zeroth order in this expansion, $V(x) = 0$ may be assumed inside the 2DES. Accordingly, the CSG theory sets the right-hand side of Eq. (1.3) zero and calculates the spatial variation of the left-hand side from electrostatic arguments. The result for the density profile of the 2DES at $B = 0$ (and $T = 0$), which can be written as

$$n_s^{\mathrm{CSG}}(x) = n_0\,(1 - d/x)^{1/2}\,\theta(x - d)\,, \tag{1.4}$$

is needed in the CSG theory to derive explicit expressions for the position and width of incompressible strips in high magnetic fields. Since the analytical result (1.4) and the assumption $V(x) = 0$ for $x > d$ violate Eq. (1.3), it is not obvious how reliable these explicit results are for finite values of the parameter $E_F/V(0)$.

The purpose of the present paper is to generalize the CSG theory and thereby to explore the range of its validity, in two respects. First, we consider (at finite temperature) a similar model with a strictly 2D distribution of charges, however, with the modification that the requirement of electrochemical equilibrium is satisfied exactly. The price of this modification will be that we have to solve the self-consistency problem numerically, even for zero temperature. Second, we consider, again at finite temperature, a realistic model with a 3D distribution of fixed and induced charges, and we show that the distribution of compressible and incompressible strips calculated for this model is also in good qualitative agreement with the CSG predictions.

In Sec. II we discuss our consistent version of the CSG model with a strictly 2D distribution of charges. In this model we complete the requirement of the electrostatics, which determines the potential resulting from a given charge distribution, by the requirement of the TFA, Eq. (1.1), which determines the charge density for a given potential distribution. Such a self-consistent electrostatic theory should be valid for all values of temperature T and of magnetic field B if potential and charge density vary on a scale d which is large compared to typical quantum lengths, such as l_m for large B and the Fermi wavelength ($\sim n_0^{-1/2} \leq 50$ nm) for small or vanishing B. For sufficiently low temperatures and high magnetic fields, this theory reproduces essentially the CSG results. As compared with the CSG theory, it has, however, the advantage that the existence of incompressible and compressible strips comes out from the self-consistent calculation, whereas in the CSG theory it is put in as an assumption, and that reasonable results can be obtained also at elevated temperatures, where such strips no longer exist.

In Sec. III we consider a realistic model of a 2DES in a wire imbedded in a sample based on a standard GaAs-$Al_xGa_{1-x}As$ heterostructure, with a corrugated top gate and a 3D distribution of donor charges.[18] Again, we treat the case of nonzero temperature and fulfill the condition of electrochemical equilibrium by means of the Thomas-Fermi approximation. We also discuss the influence of potential fluctuations in order to obtain a better understanding of the Coulomb effects inside a confined 2DEG.

II. CONSISTENT MODEL WITH PLANAR CHARGE DISTRIBUTION

A. Electrostatics

We consider a 3D model with translational symmetry in the y direction, background dielectric constants $\kappa_>$ and $\kappa_<$ in the half spaces $z > 0$ and $z < 0$, respectively, and with a charge density of the form $\rho(x)\delta(z)$ concentrated in the x-y plane. The half plane $x < 0$ is occupied by a metallic gate, so that the electrostatic potential energy of an electron $V(x,z) = -e\Phi(x,z)$, with Φ the electrostatic potential, satisfies the boundary condition $V(x,0) = V_0$ for $x < 0$, with a constant V_0. [$V_0/(-e)$ is called "gate voltage" in Ref. 15.] For $z \neq 0$, $V(x,z)$ has to satisfy the 2D Laplace equation, which is guaranteed if we write V as the imaginary part

$$V(x,z) = \mathrm{Im}\,F(\zeta) \tag{2.1}$$

of a holomorphic function F of the complex variable $\zeta = x + iz$. In the half plane $z = 0$, $x > 0$ we assume a positive background of surface charge density en_0 and a 2DES with density $n_s(x)$, so that the total surface charge

density is

$$\rho(x) = e\,[n_0 - n_s(x)] \tag{2.2}$$

and the boundary condition for the electric displacement field can be written as

$$\kappa_> \frac{\partial V}{\partial z}(x,0^+) - \kappa_< \frac{\partial V}{\partial z}(x,-0^+) = 4\pi e \rho(x)\,. \tag{2.3}$$

Since

$$\frac{\partial V}{\partial x} = \mathrm{Im}\,\frac{dF}{d\zeta}\,, \qquad \frac{\partial V}{\partial z} = \mathrm{Re}\,\frac{dF}{d\zeta}\,, \tag{2.4}$$

the boundary conditions on V define the discontinuity of the imaginary part of the auxiliary function

$$h(\zeta) = i\sqrt{\zeta}\,\frac{dF}{d\zeta} \tag{2.5}$$

along the real axis

$$\mathrm{Im}\,h(x+i0^+) = \begin{cases} r(x)\sqrt{x} & \text{if } x > 0 \\ 0 & \text{if } x < 0, \end{cases} \tag{2.6}$$

where $\sqrt{\zeta}$ is holomorphic, except the branch cut along the negative real axis ($x < 0$), and where

$$r(x) = \frac{4\pi e}{\kappa_> + \kappa_<}\,\rho(x) \tag{2.7}$$

and $\partial V/\partial z(x,-0^+) = -\partial V/\partial z(x,0^+)$ has been anticipated. The solution of our electrostatic problem is immediately obtained from

$$\frac{dF}{d\zeta}(\zeta) = \frac{-i}{\pi\sqrt{\zeta}} \int_0^\infty dx\,\frac{r(x)\sqrt{x}}{x-\zeta}\,. \tag{2.8}$$

Integration along the real ζ axis yields, for $x > 0$,

$$V(x) = V_0 - \int_0^\infty dt\,\ln\left|\frac{\sqrt{x}+\sqrt{t}}{\sqrt{x}-\sqrt{t}}\right| \frac{r(t)}{\pi}\,. \tag{2.9}$$

It is easily seen from Eq. (2.8) that the total charge $Q = \int_0^\infty dx\rho(x)$ is exactly neutralized by the induced charge in the metal gate at $x < 0$.

The integral in Eq. (2.9) has interesting analytical properties. If the total charge Q is finite, it approaches zero for $x \to \infty$, so that $V(\infty) = V(0) = V_0$. Since we require that the 2DES with bulk density $n_s(\infty) = n_0$ screens the potential at infinity, we must have $V(\infty) = 0$. According to Eq. (2.9) this is only possible if, for $x \to \infty$, $r(x) \sim V_0/\pi x$. Thus, with $n_0 = D_0 E_F$, the mere requirement of a potential step $V(0) - V(\infty) = V_0$ leads to the asymptotic behavior

$$n_s(x)/n_0 \sim 1 - d_0/2x \quad \text{for } x \to \infty\,, \tag{2.10}$$

with

$$d_0 = (2V_0/\pi E_F)\,a_0\,, \tag{2.11}$$

where

$$a_0 = (\kappa_> + \kappa_<)/4\pi e^2 D_0 \tag{2.12}$$

is the usual 2D screening length.[19,9,10] For $\kappa_> = \kappa_<$ this reduces to $a_0 = a_B^*/2$, with $a_B^* = \kappa_< \hbar^2/e^2 m^*$ the effective Bohr radius. We want to emphasize that the asymptotic relation (2.10) must hold for any value of the magnetic field strength B.

A corresponding asymptotic $1/x$ dependence of the induced electron density profile has been obtained recently by Liu and Niu, who considered a somewhat different situation with an in-plane bias on a split 2DES in the absence of a magnetic field.[20]

In the approach of CSG,[15] assuming perfect screening of the 2DES, i.e., $V(x) = 0$ for $x > d$, the electron density for $B = 0$ is given by Eq. (1.4), so that $d_0 = d$ is the depletion length ($d = 2l$ in the notation of Ref. 15). Inserting this into Eqs. (2.2), (2.7), and (2.9), one obtains $V^{\mathrm{CSG}}(x) = 0$ for $x > d$ and

$$V^{\mathrm{CSG}}(x) = V_0\left\{\frac{1}{2} - \frac{1}{\pi}\left[\arcsin\left(\frac{2x}{d} - 1\right) + \sqrt{\frac{2x}{d}\left(2 - \frac{2x}{d}\right)}\right]\right\} \tag{2.13}$$

for $0 < x < d$, in agreement with Ref. 15. Inserting this result into Eq. (1.1) in order to calculate the electron density, one gets a constant density for $x > d$ and not the input density of Eq. (1.4). Thus the CSG model for zero magnetic field is in agreement with the requirements of electrostatics, but not with that of electrochemical equilibrium, Eq. (1.3).

B. Self-consistent solution

In order to implement electrochemical equilibrium, we require that the electron density $n_s(x)$, entering Eq. (2.9) via Eqs. (2.2) and (2.7), is given by the TFA (1.1), with $V(x)$ given by Eq. (2.9). The result is in general a nonlinear integral equation for $V(x)$, which must be solved numerically. For $B = 0$ and $T = 0$, the TFA yields Eq. (1.3) if $V(x) < E_F$. This results in

$$a_0 r(x) = \min\{E_F, V(x)\}\,. \tag{2.14}$$

In the rest of this section we measure lengths in units of the screening length a_0 and energies in units of V_0. Then the self-consistency problem, Eqs. (2.9) and (2.14), depends only on the dimensionless parameter E_F/V_0, which determines the depletion length d defined by $V(d) = E_F$. If we fix an arbitrary value of d, the self-consistency problem reduces in the interval $d \le x < \infty$ to a linear integral equation for $r(x)$. Typical solutions are presented in Fig. 1. The charge density is plotted as $[n_0 - n_s(x)]/D_0 V_0$, so that it coincides with the potential $V(x)/V_0$ for $x \ge d$. The horizontal straight lines indicate the corresponding values of E_F/V_0 and, simultaneously, the background charge density in the depletion region, where $n_s(x) = 0$. From analytical considerations one

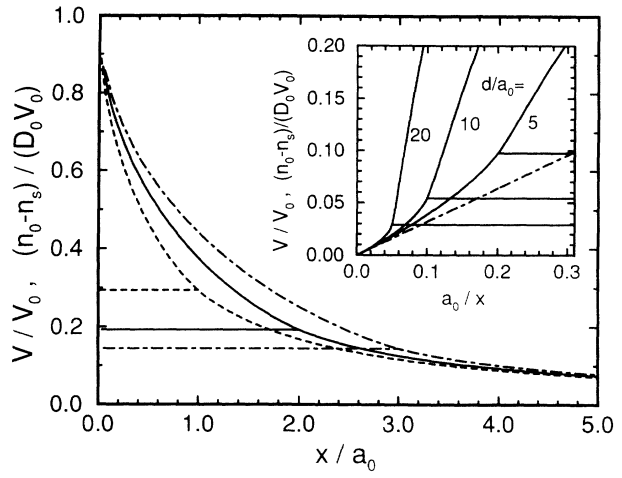

FIG. 1. Potential $V(x)$ and charge density $n_0 - n_s(x)$ in electrochemical equilibrium vs distance x from the in-plane gate, for $B = 0$ and $T = 0$ and for depletion length $d/a_0 = 1$ (dashed line), 2 (solid line), and 3 (dash-dotted line). The horizontal lines indicate the corresponding values of the Fermi energy E_F in units of the total potential variation V_0. Inset: same for $d/a_0 = 5$, 10, and 20 vs the inverse distance from the gate. The dash-dotted line indicates the asymptotic result, Eq. (2.10).

finds that, for $x \to 0$, $V_0 - V(x) \propto \sqrt{x}$, whereas $V(x)$ has a finite slope for all $x > 0$. The asymptotic behavior for large x is demonstrated in the inset of Fig. 1, where the corresponding results for three larger values of the depletion length, i.e., smaller values of E_F/V_0, are plotted versus the inverse of the distance from the in-plane gate. The dash-dotted straight line indicates the asymptotic relation (2.10).

Figure 2 shows a direct comparison of our numerical results (solid lines) with the corresponding results of Ref. 15 (dash-dotted lines). The values of the potential step V_0 and of the bulk density n_0 are the same in both cases ($E_F/V_0 = n_0/D_0V_0 = 0.0974$). The depletion length obtained from the self-consistent calculation ($d = 5a_0$) is smaller than the value d_0 ($= 6.54a_0$) of Eq. (2.11) obtained in the approach of CSG. As shown in the inset, this is true for all values of E_F/V_0. For $V_0 \gg E_F$, the dependence of the depletion length d on V_0/E_F obtained in the self-consistent model becomes linear and is well approximated by $d \approx d_0 - 2a_0$, whereas the CSG model yields the exactly linear relation $d = d_0$ with $d_0(V_0/E_F)$ given by Eq. (2.11).[17,15] Considerable deviations of the electron density profile from the predictions of Ref. 15 are obtained near the outer edge of the 2DES in a strip with a width of a few times the screening length a_0. The CSG model leads to the density profile (1.4), starting with infinite slope at $x = d_0$. This square-root singularity is an artifact resulting from the assumption of identically vanishing $V(x)$ within the 2DES right up to its edge. In our self-consistent theory $V(x)$ varies smoothly through the edge region and the density profile starts linearly with finite slope at the edge $x = d < d_0$. If the depletion length d is much larger than a_0, these differences may be considered negligible on the scale d, as argued by CSG. In this limit $E_F \ll V_0$ and the variation of the self-consistent electrostatic potential inside the 2DES is negligible on the scale of V_0, but not on the energy scale ($\sim E_F$) relevant for the 2DES.

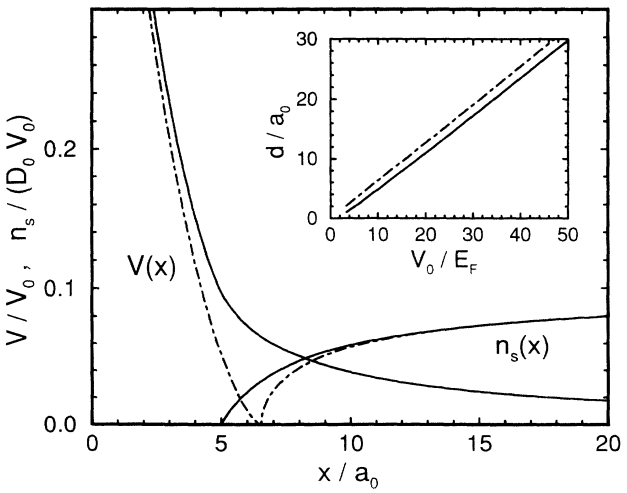

FIG. 2. Potential $V(x)$ and electron density $n_s(x)$, for $B = 0$ and $T = 0$, calculated within the electrochemical-equilibrium model (solid lines) and within the CSG model of Ref. 15 (dash-dotted lines) for the same values of potential difference V_0 and bulk electron density n_0. Inset: the corresponding results for the depletion length as a function of V_0/E_F.

To compare these results with an experimentally relevant situation, let us consider a deeply etched $Al_xGa_{1-x}As$ heterostructure, where the Fermi level is pinned by surface states in the middle of the fundamental band gap. This leads to a band bending, accompanied by a lateral depletion of the 2DES, which can be simulated by our electrostatic potential with $V_0 \sim 500$ meV. A typical value for the Fermi energy is $E_F \sim 10$ meV, resulting in $d/a_0 \approx 30$, i.e., a depletion length $d \sim 150$ nm, since $a_0 = a_B^*/2 \sim 5$ nm. In this situation the CSG approach should be well justified.

For finite magnetic field, we use in the Thomas-Fermi equation (1.1) the Landau density of states, Eq. (1.2), taking the six lowest Landau levels into account in the numerical calculations. The effect of finite temperature on the formation of incompressible and compressible strips is demonstrated in Fig. 3. The depletion length is chosen so large [$d/a_0 = 25$, $V_0/E_{F0} = 42.3$ with $E_{F0} = E_F(B = 0)$] that the CSG approach yields a good approximation to the self-consistent one for $T = 0$. The value of B is chosen to yield $\hbar\omega_c/E_{F0} = 0.423$, corresponding to a bulk filling factor $\nu_0 \equiv 2\pi l_m^2 n_0 = 4.72$. The temperature dependence of the plateaus of $V(x)$ in the compressible strips and of $n_s(x)$ in the incompressible strips is rather different. The total variation of $V(x)$ over a compressible strip is always of the order of k_BT, i.e., the (negative) slope of $V(x)$ is always finite and increases continuously with increasing temperature. Only for $k_BT/\hbar\omega_c \leq 10^{-2}$ the potential appears as flat in the compressible strips. The plateaus of the electron density in the incompressible strips, on the other hand, are absolutely flat (within the numerical accuracy) for $k_BT/\hbar\omega_c \leq 0.05$. With decreas-

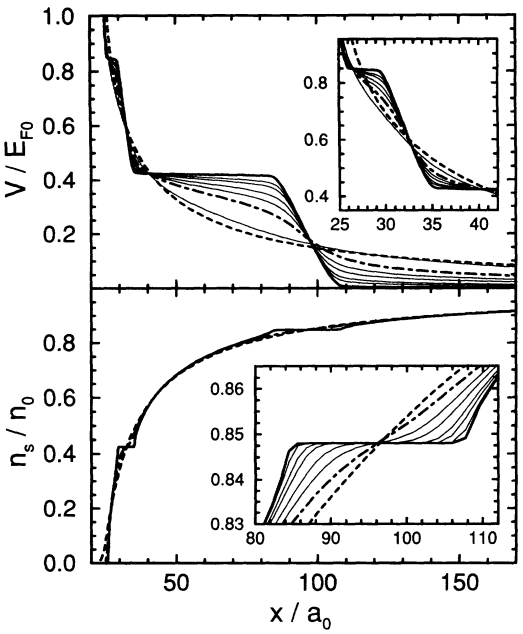

FIG. 3. Self-consistent potential (upper panel) and electron density (lower panel) for finite magnetic field ($\hbar\omega_c/E_{F0} = 0.423$, $V_0/E_{F0} = 42.3$) and several values of temperature. The thick lines refer to $k_BT/\hbar\omega_c = 0.5$ (dashed), 0.1 (dash-dotted), and 0.005 (solid), respectively. The thin solid lines in the lower inset refer to $k_BT/\hbar\omega_c = 0.07$, 0.05, 0.03, 0.02, and 0.01, and in the upper inset to 0.2, 0.07, 0.05, 0.03, and 0.02.

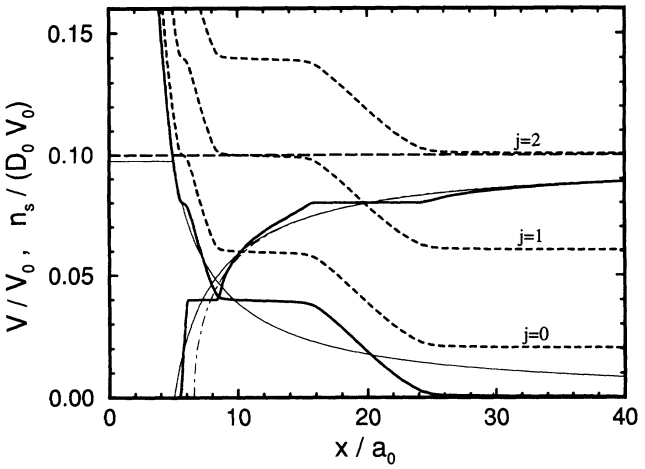

FIG. 4. Electrochemical equilibrium results for potential and electron density (solid lines) and Landau bands $j = 0$, 1, and 2 (broken lines) for finite magnetic field and temperature ($E_{F0}/V_0 = 0.097$, $\hbar\omega_c/V_0 = 0.04$, $k_BT/\hbar\omega_c = 0.01$). The long-dashed line indicates the Fermi level. Potential, electron density, and Fermi level for $B = 0$ and $T = 0$ are indicated by thin solid lines. The thin dash-dotted line is the corresponding CSG result for the electron density at $B = 0$.

ing temperature the flat regions become wider, but even at $k_BT/\hbar\omega_c = 0.005$ the full zero-temperature width is not yet reached. At $T = 0$, $n_s(x)$ enters the plateaus from both sides with vertical slope, as found in Ref. 15. Near $k_BT/\hbar\omega_c = 0.06$ the incompressible strips shrink to zero width and at higher temperatures all indications of plateau regions rapidly vanish. For $k_BT/\hbar\omega_c = 0.5$ no effect of the magnetic field is left and $V(x)$ as well as $n_s(x)$ practically coincide with the corresponding curves for $B = 0$ (not shown in Fig. 3). Compared to the $T = 0$ case, the density profile in this situation is changed only near the outer edge of the 2DES, which is softened. In the same region the values of $V(x)$ are somewhat increased.

Figure 4 shows, at a very low temperature ($k_BT/\hbar\omega_c < 0.01$), the pinning of the energy spectrum at the Fermi level and the formation of compressible strips for a smaller value of the depletion length ($d/a_0 = 5$), where the deviations from the CSG approach are noticeable and the position of the outermost compressible and incompressible strips does not agree well with the CSG prediction.

In Fig. 5 we show $V(x)$ and $n_s(x)$ obtained from self-consistent calculations for very low temperatures and for the same values of V_0 and n_0 as in Fig. 3, but for bulk filling factors near $\nu_0 = 2$. In order to exhibit the behavior far inside the 2DES, we plot the data versus the inverse distance from the metal gate. As the value $\nu_0 = 2$ is approached from above, the incompressible strip shifts away from the edge and the outer compressible strip becomes increasingly wider. As ν_0 gets smaller than 2, the incompressible strip disappears and the electrostatic potential changes dramatically. Then the screening becomes nearly perfect everywhere in the 2DES and the self-consitent result looks very similar to the CSG result for $B = 0$. It is seen that the asymptotic behavior of $n_s(x)$ for $x \to \infty$ is always given by Eq. (2.10), whereas $V(x)$ approaches zero much faster for strong magnetic fields than for $B = 0$.

Finally, we compare in Fig. 6, again for $V_0/E_{F0} = 42.3$ and for several values of the bulk filling factor, the position of the incompressible strips obtained from our self-consistent model with the analytical prediction of Ref. 15. The CSG prediction for the edges of the incompressible

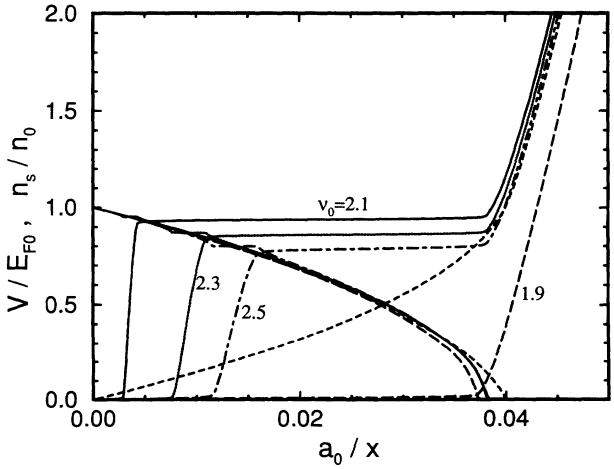

FIG. 5. Potential and corresponding electron density (same line type) for several values of the bulk filling factor close to 2 vs inverse distance from the gate. The short-dashed lines are for $B = 0$ and $T = 0$.

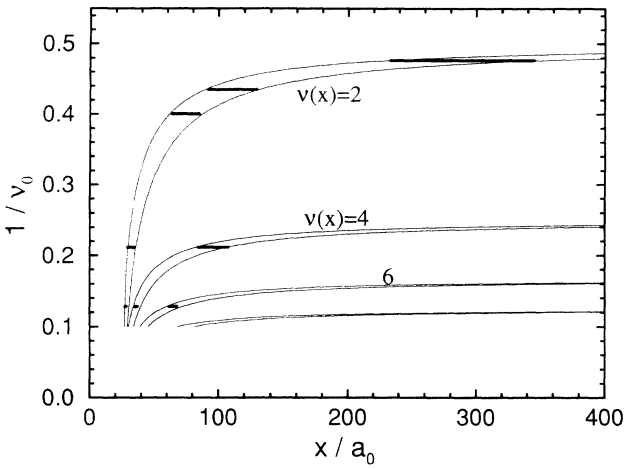

FIG. 6. Location of incompressible strips corresponding to values $\nu(x) = 2$, 4, 6, and 8 of the local filling factor (horizontal axis) at different magnetic fields, measured by the inverse bulk filling factor (vertical axis). The thin solid lines mark the analytical result of the CSG theory, the thick horizontal bars are numerical results of our self-consistent theory ($E_{F0}/V_0 = 0.0236$).

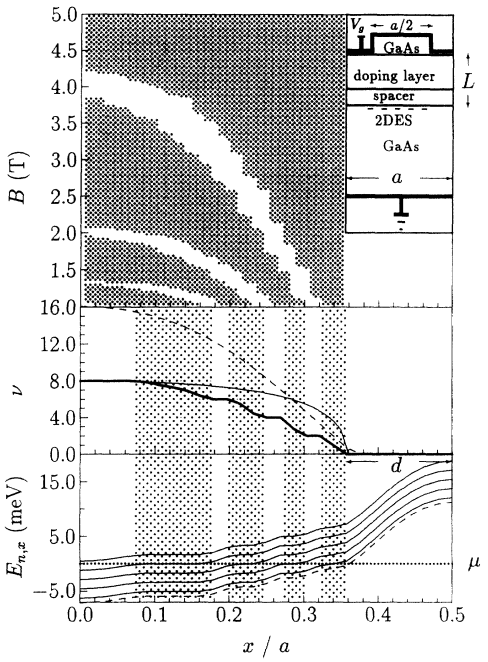

FIG. 7. Numerical results calculated for a 800 nm wide sample and a negative gate voltage of $V_g = -0.7\,\mathrm{V}$. Bottom panel: lateral dispersion of the lowest Landau bands according to the self-consistent potential (dashed line). Energies are measured relative to Fermi level μ. Middle panel: local filling factor calculated from our model for $B = 1\,\mathrm{T}$ and $T = 0.1\,\mathrm{K}$ (thick solid line) and according to Eq. (3.4) (thin solid line). The dashed line gives the local filling factor at $B = 0.5\,\mathrm{T}$ and $T = 10\,\mathrm{K}$, where no flattening out at even filling factor occurs. Even values of ν are indicated by dotted lines. Top panel: as in the two lower panels the compressible regions are shaded. Starting with the situation at $B = 1\,\mathrm{T}$ this plot shows the evolution of the incompressible strips, embedded in a compressible liquid, with increasing magnetic field.

strip with local filling factor $\nu(x_k) = g_s k$ is, in our notation and for $\kappa_> = \kappa_<$ (i.e., $a_B^* = 2a_0$), $x_k \pm \tilde{a}_k/2$, with

$$x_k = d_0/[1 - (g_s k/\nu_0)^2] \tag{2.15}$$

the position of the center and

$$\tilde{a}_k = 4x_k(g_s k a_B^*/\pi d_0)^{1/2}/\nu_0 \tag{2.16}$$

the width of the strip number k ($= 1, 2, ...$). The thin lines in Fig. 6 indicate these results for $g_s = 2$. Note that Eqs. (12) and (28) of Ref. 15 refer to the case $g_s = 1$ and $\kappa_> \ll \kappa_<$. Apparently, the agreement is astonishingly good for strips which are not too close to the outer edge of the 2DES.

III. MODEL WITH THREE-DIMENSIONAL CHARGE DISTRIBUTION

A. Model

We now consider a realistic model of a real 3D sample containing a laterally confined 2DES.[18] For technical reasons we consider a 2DES in a wire, with translational symmetry in the y direction, and we repeat the wire structure periodically in the x direction, with a sufficiently large distance between the wires, so that they do not interact with each other. The inset of Fig. 7 shows (in the x-z plane) a schematic sketch of a unit cell of this structure. The 2DES is located in the GaAs substrate near its interface (at $z = L_s$) with an $Al_xGa_{1-x}As$ layer, which behind a spacer is doped with Si donors (concentration $N_d = 10^{18}\ \mathrm{cm}^{-3}$). The periodic wire structure is defined by a corrugated (etched) cap layer (GaAs) with a x-dependent surface profile [$z = g(x)$], which is covered with a metal gate. The lateral confinement of the 2DES is determined by the electrostatic potential resulting from the gate voltage applied between the corrugated top gate and a plane metallic backgate, the charge distribution in the 2DES, and the (also inhomogeneously distributed) donor charges.[18] We take the width a of the unit cell sufficiently large so that, similar to the model discussed in Sec. II, the x dependence of the potential confining the 2DES to the wire is smooth on the scale of typical quantum mechanical lengths. Then we expect that, in a strong perpendicular magnetic field, the 2DES near an edge of the wire behaves similarly to the 2DES near the edge of a half plane, which we discussed in Sec. II.

We now sketch briefly the mathematical treatment of this model, closely following Ref. 18, to which we refer for further details. Assuming a strong confinement in the z direction, we neglect effects of higher electrical subbands and decouple the slow lateral variation of the electron density from the rapid variation in the z direction by means of a product ansatz

$$\rho_{\mathrm{FH}}(\beta, \mathbf{x}) = -e n_s(x)\, |\varphi_{\mathrm{FH}}(\beta, z)|^2\,, \tag{3.1}$$

where we describe the lowest occupied electrical subband by a Fang-Howard trial wave function

$$\varphi_{\rm FH}(\beta,z)=\left[\beta^3/2\right]^{\frac{1}{2}}\left[z-L_s\right]\exp[-\beta(z-L_s)/2]\,, \quad (3.2)$$

defined for $z>L_s$. Here L_s is the position of the interface between spacer and GaAs. To calculate the optimum value of the variational parameter β, we minimize the single-particle energy at $x=0$,

$$E_0=\left\langle\varphi_{\rm FH}(\beta,z)\left|\frac{\hbar^2}{2m^*}\frac{\partial^2}{\partial z^2}+V(x=0,z;b)\right|\varphi_{\rm FH}(\beta,z)\right\rangle\,, \quad (3.3)$$

where the Hartree contribution to V is calcutated with a Fang-Howard function as in Eq. (3.2), but with β replaced by a value b which is kept fixed. To achieve self-consistency, the stationary condition is evaluated for $\beta=b$. For a laterally homogeneous 2DES this calculation can be performed analytically and leads to the well known results.[19,21] The lateral modulation of the 2D electron density is calculated in the Thomas-Fermi approximation, Eqs. (1.1) and (1.2), where $V(\mathbf{r})$ is replaced by $V(x,\langle z\rangle)$, i.e., the potential energy of an electron is taken at the expectation value of the z coordinate ($\langle z\rangle=3/\beta$). The Landau spectrum is, of course, shifted by the energy E_0 of the lowest electrical subband defined by Eq. (3.3). This defines the charge density of the 2DES in a given potential $V(x,z)$.

As mentioned above, we also include the fixed ionization profile for the Si donors, which has been calculated self-consistently at elevated temperatures, when the electrons in shallow and deep donor states within the $Al_xGa_{1-x}As$ doping-layer behave like mobile charges and screen effectively the electrostatic potential imposed by a top gate. This screening and, in addition, the exponential decay of short-range lateral potential fluctuations due to Poisson's equation, smoothens the effective lateral potential confining the 2DES in the x direction, although the etching pattern on top of the heterojunction may be extremely sharp.[18]

To achieve electrochemical equilibrium we proceed as follows. We calculate the potential distribution from Poisson's equation with the charge density of the 2DES and the donor distribution as source terms and with the boundary conditions imposed by the metallic top and back gates. Then we use this $V(x,z)$ to calculate the electron density anew and we iterate the process until convergency is achieved. Using the TFA with the Landau density of states, Eq. (1.2), we thus calculate the peculiar screening behavior of the 2DES at low temperatures and high magnetic fields.

B. Results

The lowest panel of Fig. 7 shows the self-consistent potential energy of an electron as well as the five lowest Landau bands for $B=1\,\mathrm{T}$ and $T=0.1\,\mathrm{K}$. The gate voltage applied between the corrugated top gate and the plane backgate is $V_g=-0.7$ V, resulting in a total variation $V_0\approx 18$ meV of the electrostatic potential energy in the plane of the 2DES, which is not very much larger than the Fermi energy $E_F\approx 7.1$ meV. The pinning of different Landau bands at the Fermi level is clearly resolved. These compressible regions are well separated by incompressible strips with even (g_s=2) filling factor, which can be identified in the panel above. There we have plotted the local filling factor $\nu(x)=2\pi l_m^2 n_s(x)$, whose behavior, as in the 2D model of Sec. II, is complementary to that of the potential. The strips with flat potential coincide with variable filling factor, while the adjacent incompressible strips with constant filling factor show a nonzero gradient in the electrostatic potential. The dashed curve indicates the local filling factor for $B=0.5\mathrm{T}$ and $T=10$ K and demonstrates the vanishing of incompressible regions at higher temperature.

Quantitative predictions of the CSG theory as well as its self-consistent version proposed in Sec. II should fail if the depletion length d is comparable with the distance of the 2DES from the top gate L (see the inset of Fig. 7). The parameters of Fig. 7 are chosen so that the ratio of the depletion length d to the gate distance L is 0.9, i.e., the 2DES and the gate can hardly be assumed to be located in the same plane. In addition to the numerically calculated local filling factor (thick solid line) we plotted the result of the (here hardly justified) CSG model at $B=0\,\mathrm{T}$, but for a finite wire [see, e.g., Eq. (6) of Ref. 16] in the way that the depletion length d and the filling factor in the "bulk" $\nu(0)$ fits our data,

$$\nu(x)=\frac{\nu(0)}{1-2d/a}\left[\frac{(d-a/2)^2-x^2}{a^2/4-x^2}\right]^{\frac{1}{2}}\,. \quad (3.4)$$

The positions of incompressible strips would be expected where the CSG curve crosses the horizontal dotted lines of even-integer filling factor, in obvious disagreement with our self-consistent results. The situation is similar to that of Fig. 2, where we compared the CSG result with its self-consistent generalization, assuming the same values of the bulk density n_0 and of the total potential step V_0 for both. If we had assumed instead the same values of n_0 and of the depletion lenght d, i.e., a smaller value of V_0 for the CSG curves, then the CSG result for the electron density $n_s(x)$ would always be larger than the self-consistent-screening result and would increase much more rapidly with increasing distance from the edge. This means that in the self-consistent theory screening of the electrostatic potential in the edge region is less effective and the electrons are repelled more effectively from the edge than in the CSG model, which *assumes* perfect metallic screening by the 2DES. Whereas in Fig. 2 differences between the CGS model and the self-consistent approach become visible because the depletion length d is not much larger than the screening length a_0, the discrepancies seen in Fig. 7 originate also from the fact that d is not (much) larger than the distance L of the gate from the plane of the 2DES. Apparently the smooth confinement potential produced by the remote charges is only poorly screened by the 2DES so that it penetrates into a broad edge region of the wire, resulting there in a much smaller electron density than expected from a

model assuming perfect screening. As a consequence, the self-consistent 3D calculation yields incompressible strips of considerably larger width and at a considerably larger distance (on the scale of d) from the edge than is predicted by the analytic CSG model.[15,16]

As a guide for the eye the compressible regions in Fig. 7 are shaded. Starting with the pattern at $B = 1$ T, the uppermost panel gives an impression of the further evolution of the position of compressible and incompressible strips with increasing magnetic field up to 5 T. The fuzzy boundaries of the shaded areas are due to the coarse mesh of B values and, even more important, of the x values used in our numerical calculations. Note that all the characteristic features of this pattern agree *qualitatively* with those of Fig. 6, obtained within the simplified model of Sec. II for the edge region of a semi-infinite 2DES. *Quantitatively*, however, the wire version of the latter would lead to a pattern of unshaded strips which are nearly horizontal in a broad central region and then fall off very rapidly in a narrow region near the edge of the wire, with a much steeper slope than seen in Fig. 7. This is a direct consequence of the fact that, for zero temperature, the electron density profile in the perfect-screening approximation increases near the edge with a much steeper slope than the self-consistent result.

We want to emphasize the following most remarkable features. On the one side the width of the incompressible strip in the center ("bulk") is much larger than the width of those located close to the edge. But incompressible bulk channels can exist only in a narrow range of magnetic fields. In the semi-infinite model of Sec. II the width of this range shrinks to zero. For most magnetic fields the bulk region is compressible. In general, if B is swept to higher values, the innermost incompressible strip will vanish and the subsequent strips of even-integer filling factor move from the edges towards the middle of the sample, eventually merging into a new incompressible bulk channel. Especially at filling factors larger than 2, this channel immediately disappears after further increasing the magnetic field by a rather small amount. This repeats until the last incompressible bulk channel has disappeared and, within our model assumptions neglecting spin splitting and many-particle correlation effects, the whole sample becomes compressible.

The width of the incompressible strips decreases if the width of the wire, i.e., the period a of our array model, is reduced and the confinement potential becomes steeper. For $a \leq 600$ nm we could hardly resolve any incompressible strips within the accuracy of our calculation.

Figure 8 shows results for a broader wire ($a = 2\,\mu$m) and a smaller bulk filling factor, where only one incompressible strip exists in each edge region and the center region is compressible. To demonstrate the "perfect screening" property of our 2DES in the compressible regions, we also performed the calculation with an additional small external potential fluctuation $\delta V(x) = (\delta V/2)\cos(2\pi x/\lambda)$ with a period much smaller than the wire width but somewhat larger than the magnetic length ($\lambda/l_m = 11/4$ and $\delta V/\hbar\omega_c \approx 1/7$). The results are also shown in Fig. 8. It is seen that pinning of the energy spectrum at the Fermi level, accompanied by the characteristic flattening of the potential in the compressible strips, survives, as does the region of constant filling factor. Apparently the perfect screening is the consequence of a pronounced redistribution of the electron density in the compressible area as response to the additional potential fluctuation. Note that the unequality $\delta V > k_B T$ holds. With increasing amplitude of the perturbing potential the density modulation will become larger until the local filling factor approaches somewhere in the compressible region an even-integer value and the perfect screening breaks down. A large-amplitude perturbation with smoothly varying potential will behave similar to the confinement potential at the edge of the 2DES and introduce new compressible and incompressible regions. If, in a real sample, such a perturbation is localized and located far from the edge, the surrounding strips will be closed and act as bound states.

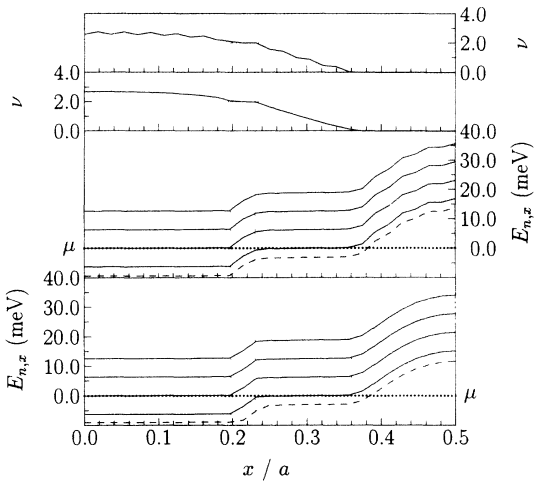

FIG. 8. Comparison between a "dirty" sample, simulated by a potential fluctuation $\delta V(x) = (\delta V/2)\cos(8\pi x/11 l_m)$ with $\delta V = 0.85$ meV, and a clean one ($\delta V = 0$), for parameters $a = 2\,\mu$m, $B = 3.7$ T, $T = 0.1$ K, and $V_g = -1.2$ V (chosen to keep the ratio of a and the width of the 2DES close to that of Fig. 7). The local variation of the potential profile and the dispersion of Landau bands (the two lower panels) as well as the local filling factors (upper panels) are shown. The right scale refers to the perturbed 2DES.

C. Implications for magnetoconductance

Recently Chklovskii, Matveev, and Shklovskii[16] suggested to generalize the Landauer two-terminal conductance formula for a wire to the case of noninteger filling factor within the bulk as

$$G = \frac{e^2}{h}\nu(0)\,, \tag{3.5}$$

where $\nu(0)$ is the maximum of the local filling factor $\nu(x)$. In Fig. 9 the magnetic-field dependence of $1/\nu(x)$ is plotted for various x values along the cross section of the $2\,\mu$m wide sample (for $\delta V = 0$). Incompressible strips lead to plateaus in this plot. The width of these plateaus

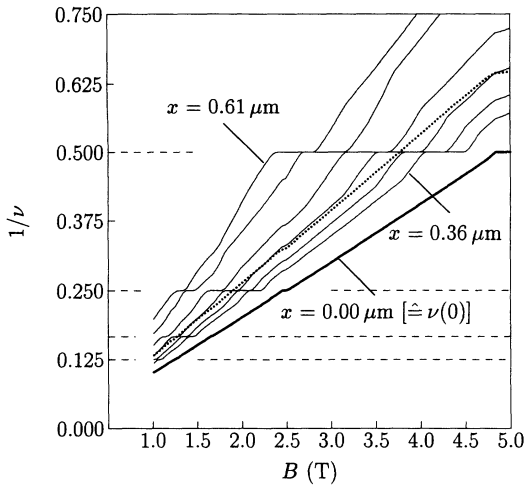

FIG. 9. Magnetic field dependence of the inverse local filling factor at different equidistant positions close to the sample edge ($|x|$ =0.36–0.61 μm). In addition, the inverse of the filling factor taken at the middle of the sample ($x = 0\,\mu$m) is shown (thick line). The dotted line corresponds to the averaged filling factor defined in (3.6). Parameters are the same as in Fig. 8.

decreases as x moves from the edge towards the center of the wire ($x = 0$), where the plateaus are narrowest. As is seen from Fig. 9, Eq. (3.5) leads to extremely narrow quantum Hall plateaus for our wires, similar to the narrow plateaus due to edge states obtained in the single-electron picture.[4] Thus, in order to understand, on the basis of this suggestion, the pronounced quantum Hall plateaus seen in transport experiments on quantum point contacts (see, e.g., Refs. 22 and 3) and Hall bars,[5] one must, in addition, invoke pinning of the Fermi energy by some kind of localized states. Without any additional assumptions, Eq. (3.5) cannot explain the experimentally observed width of quantum Hall plateaus and the situation is just as in the single-electron picture, which does not take into account any screening effects. The plateau width read off from Fig. 9 is even larger than one would expect for a sample with constant mean electron density in the wire. To elucidate this point, the dotted line shows the inverse of the mean filling factor $\bar{\nu} = 2\pi l_m^2 \bar{n}_s$ defined with the mean electron density

$$\bar{n}_s = \frac{1}{a}\int_{-a/2}^{a/2} n_s(x)dx\,. \tag{3.6}$$

For constant $\bar{n}_s$ the dotted line would have to be straight. In our B sweep, however, we fix the gate voltage and not the density, just as in the experiments. As a consequence, the mean electron density in the wire, but also the width of the Fang-Howard function in z direction and the corresponding electrical-subband energy E_0 of Eq. (3.3) become B dependent. In principle, and for oversimplified not self-consistent models, such a B dependence of the density may lead to broad quantum Hall plateaus ("reservoir model"; see, e.g., Zawadski and Kubisa[23]). We have calculated the variation of the mean 2D electron density within our self-consistent approach. It turns out to be very small (of the order of 1%) and cannot lead to any significant consequences like a realistic plateau width of the quantized Hall resistance. This very small variation of $\bar{n}_s$ as a function of B is in total agreement with results of previous self-consistent calculations for heterostructures with a *homogeneous* 2DES,[21] where no confinement in lateral directions was included and acceptor states in the GaAs substrate were treated as a reservoir. The weak B dependence of $\bar{n}_s$ leads to the tiny steps seen in the dotted curve of Fig. 9, which refers to the mean filling factor $\bar{\nu}$. Since these steps are closely correlated with the narrow plataus seen in $1/\nu(0)$, the latter, and according to Eq. (3.5) also the plateaus of the conductance, would essentially shrink to zero if $\bar{n}_s$ instead of V_g would be kept constant during the B sweep.

IV. CONCLUSIONS

Using the Thomas-Fermi approximation for the electron density distribution in electrochemical equilibrium, we have investigated the screening of slowly varying electrostatic fields by a two-dimensional electron system in a perpendicular magnetic field of arbitrary strength and at arbitrary temperature. We considered two different models for GaAs-(AlGa)As heterostructures containing a 2DES with translation symmetry in one direction. For the first model, which assumes the metal gate and all charges to be in the plane of the 2DES, Poisson's equation can be solved analytically, so that the requirement of electrochemical equilibrium reduces to a one-dimensional nonlinear integral equation. For the second model, with a three-dimensional arrangement of gates and space charges, this is not possible and the full, effectively two-dimensional self-consistency problem must be solved numerically. Both models yield qualitatively the same results and lead to the same picture of screening. In a strong magnetic field and at low temperatures ($k_BT/\hbar\omega_c \leq 0.01$), the 2DES can be divided into alternating incompressible and compressible regions. In the compressible regions the screening is "perfect" and the electrostatic potential is constant, while in the incompressible regions the electron density is constant, so that they do not contribute to screening. The results for the electron density profile $n_s(x)$, and in particular for position and width of the incompressible regions, obtained from the first model is in excellent quantitative agreement with the corresponding results of Ref. 15, provided that the depletion length d is much larger than the screening length a_0 for $B = 0$ or that the distance from the edge is large enough $x \gg a_0$. The results for the second model demonstrate that, for realistic sample geometries, considerable deviation (on the scale of d) of these positions and widths from the predictions of Ref. 15 or its wire version, Ref. 16, must be expected if d is not much larger than the distance L of relevant gate or space charges from the plane of the 2DES.

At elevated temperatures the concept of incompressible and compressible regions breaks down and the approach of Ref. 15 becomes meaningless, whereas our ap-

proach is still valid. We have shown that this happens at a temperature where k_BT exceeds a few percent of the cyclotron energy $\hbar\omega_c$. Below this temperature, the simple analytical theory of Ref. 15, despite its somewhat oversimplifying assumptions, yields excellent results if the conditions $d \gg a_0$ and $d \gg L$ are fulfilled. This is an important result of our work, which does not *assume* the existence of the compressible and incompressible regions as CSG do, but *calculates* them from a more general, self-consistent approach.

The condition $d \gg L$ may, however, not hold for a given sample and then the quantitative predictions of Ref. 15 will also not apply. We have presented such an example for a gated structure, where a large gate voltage applied in the vertical direction produces only a relatively small lateral potential variation V_0 in the plane of the 2DES, so that the relevant ratio E_F/V_0 is not very small. On the other hand, the predictions of Ref. 15 may apply well to deeply etched samples (even without top gate) where an etched surface produces the lateral confinement of the 2DES and the Fermi level is pinned by surface states in the middle of the fundamental band gap, which leads to a large lateral band bending. This may be well described by a large potential variation in the plane of the 2DES, $V_0 \sim 0.5$ eV $\gg E_F \sim 10$ meV, and therefore a large depletion length $d \sim 100$ nm $\gg a_0 \approx 5$ nm.

In conclusion, our calculations essentially confirm the general picture of screening in the quantum Hall regime propagated by Chklovskii, Shklovskii, and Glazman, and, in particular, they confirm the formation of alternating incompressible and compressible strips in regions of varying electron density, e.g., in edge regions. The interpretation of some recent experiments on Hall bar samples[7,8] seems to be possible only within this picture and strong evidence for the existence of incompressible strips has been found.[7] Also tunnel-spectroscopy experiments on quantum dot systems[24] and related Hartree calculations[24,25] support this picture of screening. Therefore, it seems necessary to comment on a recent Hartree calculation by Brey, Palacios, and Tejedor,[26] who find pinning of the Landau bands at the Fermi energy, but no noticeable incompressible regions of constant electron density. The reason for this finding is the absence of long-ranged smoothly varying electrostatic potentials in their model, which defines a quantum wire by infinite-step potentials at the edges and a trapezoidal distribution of positive background charges being locally neutralized by the 2DES. In this model the minimization of electrostatic energy forces the electron density to follow closely that of the background charges, resulting in narrow incompressible strips (a few magnetic lengths wide) between broad compressible strips in which adjacent Landau bands are pinned at the Fermi level. This situation is very different from the one considered in our model, where uncompensated (depletion) charges produce a smoothly varying electrostatic potential which bends the Landau bands and leads to broad incompressible strips. Thus the experiments probing the existence of incompressible strips[7] indicate that a (deeply etched) surface serving as a lateral confinement of a 2DES accommodates charged surface states, leading to strong band bending and a large depletion length, and that it cannot be well described by a simple step potential.

ACKNOWLEDGMENTS

We would like to thank R.J. Haug and N.B. Zhitenev for helpful discussions and F. Stern and R.J. Haug for a critical reading of the manuscript.

[1] M. Büttiker, IBM J. Res. Dev. **32**, 317 (1988).
[2] C.W.J. Beenakker and H. van Houten, in *Solid State Physics*, edited by H. Ehrenreich and D. Turnbull (Academic Press, San Diego, 1991), Vol. 44, p. 1.
[3] H. van Houten and C.W.J. Beenakker, in *Semiconductors and Semimetals*, edited by M. Reed (Academic Press, San Diego, 1992), Vol. 35, p. 9.
[4] M. Büttiker, in *Semiconductors and Semimetals* (Ref. 3), p. 191.
[5] R.J. Haug, Semicond. Sci. Technol. **8**, 131 (1993).
[6] G. Müller, D. Weiss, S. Koch, K. von Klitzing, H. Nickel, W. Schlapp, and R. Lösch, Phys. Rev. B **42**, 7633 (1990).
[7] N.B. Zhitenev, R.J. Haug, K. von Klitzing, and K. Eberl, Phys. Rev. Lett. **71**, 2292 (1993).
[8] S.W. Hwang, D.C. Tsui, and M. Shayegan, Phys. Rev. B **48**, 8161 (1993).
[9] J. Labbé, Phys. Rev. B **35**, 1373 (1987).
[10] U. Wulf, V. Gudmundsson, and R.R. Gerhardts, Phys. Rev. B **38**, 4218 (1988).
[11] U. Wulf and R.R. Gerhardts, in *Physics and Technology of Submicron Structures*, edited by H. Heinrich, G. Bauer, and F. Kuchar, Springer Series in Solid-State Sciences Vol. 83 (Springer-Verlag, Berlin, 1988), p. 162.
[12] S. Luryi, in *High Magnetic Fields in Semiconductor Physics*, edited by G. Landwehr, Springer Series in Solid-State Sciences Vol. 71 (Springer-Verlag, Berlin, 1987), p. 16.
[13] A.L. Efros, Solid State Commun. **67**, 1019 (1988).
[14] A.L. Efros, Solid State Commun. **70**, 253 (1989).
[15] D.B. Chklovskii, B.I. Shklovskii, and L.I. Glazman, Phys. Rev. B **46**, 4026 (1992); **46**, 15 606 (1992).
[16] D.B. Chklovskii, K.A. Matveev, and B.I. Shklovskii, Phys. Rev. B **47**, 12 605 (1993).
[17] L.I. Glazman and I.A. Larkin, Semicond. Sci. Technol. **6**, 32 (1991).
[18] K. Lier and R.R. Gerhardts, Phys. Rev. B **48**, 14 416 (1993).
[19] F. Stern and W.E. Howard, Phys. Rev. **163**, 816 (1967).
[20] X. Liu and Q. Niu, Phys. Rev. B **46**, 10 215 (1992).
[21] V. Gudmundsson and R.R. Gerhardts, Phys. Rev. B **35**, 8005 (1987).
[22] B.J. van Wees, H. van Houten, C.W.J. Beenakker, J.G.

Williamson, L.P. Kouwenhoven, D. van der Marel, and C.T. Foxon, Phys. Rev. Lett. **60**, 848 (1988).

[23] W. Zawadzki and M. Kubisa, in *High Magnetic Fields in Semiconductor Physics III*, edited by G. Landwehr, Springer Series in Solid-State Sciences Vol. 101 (Springer-Verlag, Berlin, 1992), p. 187.

[24] P.L. McEuen, E.B. Foxman, J. Kinaret, U. Meirav, M.A. Kastner, N.S. Wingreen, and S.J. Wind, Phys. Rev. B **45**, 11 419 (1992).

[25] I.K. Marmorkos and C.W.J. Beenakker, Phys. Rev. B **46**, 15 562 (1992).

[26] L. Brey, J.J. Palacios, and C. Tejedor, Phys. Rev. B **47**, 13 884 (1993).